# ATTITUDE CONTROL OF GEOSTATIONARY SATELLITES WITH MINIMAL USE OF GYROSCOPES

**Michael Surauer, Peter Zentgraf, Walter Fichter**

*Dornier Satellitensysteme GmbH, P.O. Box 80 11 69, D-81663 Munich, Germany*
*Phone: (0049) 89/607 28154, Fax: (0049) 89/607 23583*
*e-mail: Peter.Zentgraf@space.otn.dasa.de*

ABSTRACT

An attitude control system of a geostationary satellite is described which does not use gyros during acquisition modes and which uses one single gyro during the apogee boost mode.

As far as the acquisition modes are concerned, the angular rates can be estimated straight forward from the Euler equation, when the satellite does not only rotate about the sunline but also transversal to it. However, in steady state only the absolute value of the sunline angular rate is estimated directly. The sign of the sunline rate can be derived from this absolute value and its derivative.

In the apogee boost mode, the required 3-axis attitude information can be derived from Sun sensor measurements and a gyro, if the gyro axis is not aligned with the Sun vector.

## 1. INTRODUCTION

Gyros are commonly used as sensors for the attitude and orbit control system of satellites. They provide not only very accurate rate information, but also attitude information can be derived e.g. when using a strap-down algorithm or the gyro-compass effect (in low orbits). However, there are two major reasons to avoid the use of gyros: First, reliable gyros are expensive, and second, a significant number of gyro failures have been reported in the past years.

In the case of a geosynchronous communication satellite, the accumulated operational time of a gyro is relatively small. They are usually used only for rate control purposes during Sun- and Earth acquisition modes, and for deriving the inertial attitude with a strap-down algorithm, during the apogee boost maneuvers. The normal mode and station keeping maneuvers are usually based on optical sensor information only (Sun- and Earth sensor).

Because of the disadvantages described above, it is desireable to have control algorithms and strategies available, that do not rely on any measured rate information in order to eliminate gyros as far as possible. Such algorithms and strategies were developed at Dornier Satellitensysteme GmbH for the attitude and orbit control system AOCS3000. This system was originally developed to be used for geosynchronous missions, but it can also be adapted to a number of other mission profiles.

With the new algorithms it is now possible to perform the Sun- and Earth acquisition modes without any gyro information. This means, once a satellite reaches the geostationary orbit, which is shortly after the launch, it does not rely on gyro information at all, even in the emergency case. As for the apogee boost maneuvers, it depends on the actual configuration of the satellite (orientation of the apogee boost motor), whether an additional sensor is needed or not. An additional sensor can either be a single-axis Earth sensor or at least one additional single-axis gyro.

This paper first presents the baseline equipment configuration of the AOCS3000. Then, the different operational modes are outlined for a geosysnchronous mission. In the main part (section 4), gyroless Sun and Earth acquisition modes are explained in detail, and then the principles of a single gyro and gyroless apogee boost mode are shown.

## 2. SATELLITE SENSOR/ACTUATOR CONFIGURATION

A typical satellite with deployed antennas and solar panels with body coordinate system (x, y, z) is shown in figure 1. The relevant AOCS equipment is described from the AOCS 3000-program [1].

It consists of 2 Earth sensors, 8 Sun sensors, 4 large reaction wheels and 14 10-N-thrusters. A gyro could be used in transfer orbit (TO) for the apogee boost maneuver which is discussed in section 4.

*Proceedings Third International Conference on Spacecraft Guidance, Navigation and Control Systems, ESTEC, Noordwijk, The Netherlands, 26-29 November 1996, ESA SP-381 (February 1997)*

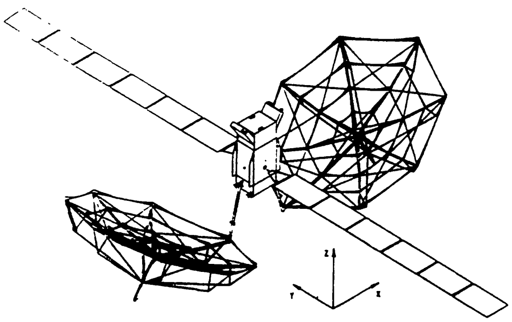

Figure 1: Satellite and body coordinate system.

*2.1 Sensors*

Two Earth sensors (one main, one redundant) are located in direction of the +z-axis.

The Sun sensors are located and oriented in such a way that a complete coverage about the y-axis is achieved in TO when the antennas are stowed. Each Sun sensor head has a FOV of ± 50 degrees.

*2.2 Actuators*

Four reaction wheels (figure 2) provide angular momentum stiffness and 3-axis torque capabilty in nominal configuration as well as in case of any failed wheel. The wheels can produce a maximum torque of 75 mNm, and their speed range is from 0 until ± 6000 rpm.

14 10-N-thrusters are divided into four sets (A, B, C, D) as shown in figure 3. This configuration guarantees positive and negative control torques about all body axes.

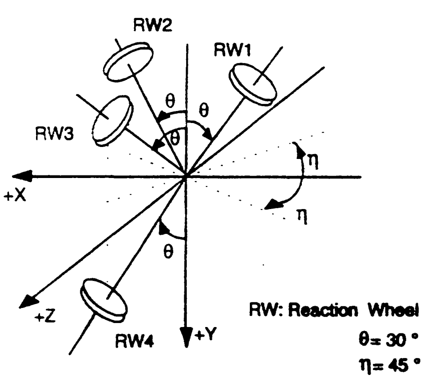


Figure 2: Reaction wheel assembly.

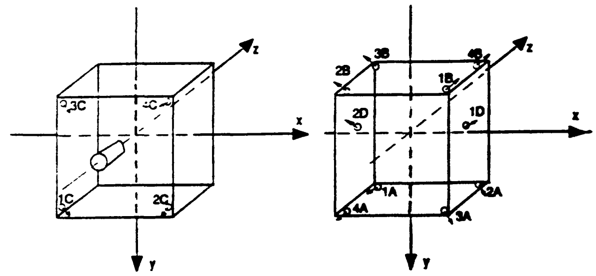

Figure 3: Thruster arrangement.

## 3. OVERVIEW ON OPERATIONAL MODES

In this section, only the principal operational modes and the necessary information for the control system provided by sensors and estimators are presented [1].

*3.1 Transfer orbit*

The sequence of events is Sun acquisition mode (SAM), Earth acquisition mode (EAM) and apogee boost mode (ABM) (figure 4).

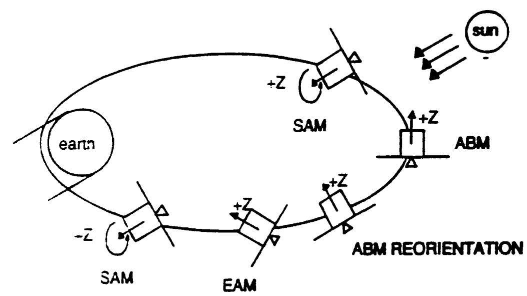


Figure 4: Sequence of events in transfer orbit.

*Sun acquisition mode.* The objective of this mode is to bring the satellite from an arbitrary initial condition to a Sun pointing attitude. The desired principal axis points to the Sun and the satellite rotates about the sunline with a constant rate. As for the measurement signals, the controller requires the Sun vector in body axes, as well as the Sun vector velocity and the acceleration. It is shown, that angular rates can be computed from Sun sensor signals, wheel angular momentum and the inertia matrix.
*Earth acquisition mode.* This mode aims at requiring the Earth from an initial Sun pointing state, in order to get the satellite 3-axis stabilized. This is achieved by commanding a new appropriate Sun reference vector, and rotation about the sunline guarantees Earth presence. The necessary measurement signals are the Sun vector, and the first and second derivative. When the Earth is found, the complete attitude is known and 3- axis attitude control yields the body z-axis pointing towards the Earth center.

*Apogee boost mode.* This mode starts with an Earth pointing attitude (x-axis in flight direction, z-axis points towards Earth) and rotates towards a new inertial reference attitude in order to align the thrust vector with the desired thrust direction, requiring Sun sensor signals and a single gyro. Then, the boost motor which is located in -z-direction will be fired.

### *3.2 Geostationary Orbit*

EAM and SAM have in geostationary orbit (GEO) the same controller structure and mode logic as in TO. However, due to the deployed panels the moment of inertia changes and structural flexibilities must be taken into account. Therefore, the controller parameters are chosen accordingly.

The remaining operational modes considered are station keeping mode and normal mode.

*Station keeping mode.* The objective of this mode is to perform orbit control, i.e. North/South or East/West maneuvers, by firing the thrusters as well as attitude control using the wheels. Only Earth and Sun sensor measurements are necessary, gyros are used for backup [1, 2].

*Normal mode.* The large reaction wheels RW1 and RW2 in figure 2 run at bias speeds in order to establish an angular momentum pointing in negative y-axis. Attitude control is based on 3-axis measurement from the Earth and Sun sensors except in colinearity regions and eclipse, where an estimated yaw attitude is derived from an observer. But even if the Sun sensors fail, the mode performance is maintained using this observer and a torque estimation- and compensation technique. The wheels as actuators provide continuous 3-axis control.

## 4. CONTROL CONCEPTS

In this section, the control concepts of the SAM, EAM and ABM are explained.

### *4.1 Sun Acquisition Mode*

As already mentioned, the objective of the SAM is to make the satellite point with a desired axis towards the Sun and rotate about the sunline with a desired angular rate. The challenge is thereby not to use gyro measurements, i.e. on first glance the angular rates are unknown.

The control problem is divided into two parts. First, a pure Sun vector control loop is designed with Sun sensor measurements only. It can be shown, that a stable sunline rate control loop does not influence the stability of the Sun vector control loop. The angular rates are estimated from the closed loop system equations. Then, the sunline rate control loop is designed.

*Sun vector control.* The satellite rigid body motion can be described by the Euler equation expressed in body coordinates

$$I\dot{\underline{\omega}} + \underline{\tilde{\omega}}(I\underline{\omega} + \underline{h}) + \dot{\underline{h}} = \underline{\tau}\,, \qquad (1)$$

where

| | |
|---|---|
| $I$ | moment of inertia matrix, |
| $\underline{\omega}$ | angular rate vector, |
| $\underline{h}$ | wheel angular momentum vector, |
| $\underline{\tau}$ | external torque vector, |

and it is asumed that $\dot{\underline{h}} = \underline{0}$. On top of a letter, denotes the time derivative and '~' denotes the skew symmetric cross product matrix of a vector.

A tranversal angular rate with respect to the sunline can be derived from the well-known relation

$$\dot{\underline{s}} = -\underline{\tilde{\omega}}\,\underline{s} \qquad (2)$$

to be

$$\underline{\omega}_t = \underline{\dot{\tilde{s}}}\,\underline{s}\,. \qquad (3)$$

However, the angular rate component in sunline direction,

$$\underline{\omega}_l = \underline{s}\,\omega_l\,, \qquad (4)$$

remains unknown.

Multiplying eq. (1) from the left with $\underline{\tilde{s}}I^{-1}$ and inserting the differentiated eq. (2) yields after some manipulation

$$\ddot{\underline{s}} - \underline{\dot{\tilde{s}}}\,\underline{\dot{\tilde{s}}}\,\underline{s} = \underline{\tilde{s}}I^{-1}(\underline{\tau}_c - \underline{\tilde{\omega}}_t I \underline{\omega}_t - \underline{\tilde{\omega}}_t \underline{h} + \underline{d})\,, \qquad (5)$$

where $\underline{\tau}_c = \underline{\tau}$ is the external control torque provided by the thrusters and

$$\underline{d}(\underline{s},\dot{\underline{s}}) := -(\underline{\tilde{\omega}}_t I \underline{s} - \underline{\tilde{s}} I \underline{\omega}_t + \underline{\tilde{h}}\,\underline{s} - I\dot{\underline{s}})\,\omega_l - \underline{\tilde{s}} I \underline{s}\,\omega_l^2 \qquad (6)$$

comprises all terms with the unknown scalar sunline rate $\omega_l$. As long as $\omega_l$ is in a stable control loop system it can be considered as a time varying, bounded parameter. The terms with the known angular rate components $\underline{\omega}_t$ in eq. (5) can be compensated by

$$\underline{T}_c := I^{-1}(\underline{\tau}_c + \underline{\tilde{\omega}}_t I \underline{\omega}_t + \underline{\tilde{\omega}}_t \underline{h}) \qquad (7)$$

to yield

$$\ddot{\underline{s}} - \dot{\tilde{\underline{s}}}\tilde{\underline{s}}\underline{s} = \tilde{\underline{s}}(\underline{T}_c + I^{-1}\underline{d}) \,. \tag{8}$$

The control torque $\underline{T}_c$ in eq. (7) is now split into a transversal component $\underline{T}_t$ and a longitudinal component $\underline{T}_l$ with respect to the sunline,

$$\underline{T}_c = \underline{T}_l + \underline{T}_t \,, \tag{9}$$

where only $\underline{T}_t$ has an influence in eq. (8) because the Sun vector $\underline{s}$ is parallel to $\underline{T}_l$.

For Sun vector control, only two Sun vector components need to be considered, since the magnitude of the third component is determined by the other two. In the control law proposed here the y-component is continously controlled, because the solar panels are along the body y-axis (figure 1) and for power supply the Sun vector should be in the x-z plane of the body coordinate system.

Next, the control laws for the x-, y-, and z-component (components are denoted through indices) of the Sun vector are given, such that the Sun vector is driven towards a reference Sun vector $\underline{s}_r$, while the controller gains $k_{px}$, $k_{py}$, $k_{pz}$ and $k_{dx}$, $k_{dy}$, $k_{dz}$ amplify the feed back signals $(\underline{s} - \underline{s}_r)$ and $\dot{\underline{s}}$ :

1. Control law for $s_y$:

$$T_{tx} = -\frac{s_z}{s_x^{\,2} + s_z^{\,2}}\left[\left(s_y - s_{ry}\right)k_{py} + \dot{s}_y k_{dy}\right] \tag{10}$$

$$T_{tz} = +\frac{s_x}{s_x^{\,2} + s_z^{\,2}}\left[\left(s_y - s_{ry}\right)k_{py} + \dot{s}_y k_{dy}\right] \tag{11}$$

Note that the denominator in eqs. (10, 11) cannot become zero because the Sun sensors are arranged about the body y-axis such that Sun presence along the y-axis cannot be detected.

2. Control law for $s_x$:

$$T_{ty} = \frac{1}{s_z}\left[\left(s_x - s_{rx}\right)k_{px} + \dot{s}_x k_{dx} + s_y T_{tz}\right] \tag{12}$$

This control law is applied when

$$|s_x| < |s_z| \,. \tag{13}$$

3. Control law for $s_z$:

$$T_{ty} = -\frac{1}{s_x}\left[\left(s_z - s_{rz}\right)k_{pz} + \dot{s}_z k_{dy} - s_y T_{tx}\right] \tag{14}$$

This control law is applied when

$$|s_z| \le |s_x| \,. \tag{15}$$

In order to set up the closed loop system equations, the state vector

$$\underline{s}_2^{\,T} = [s_i \, s_y] \tag{16}$$

is defined where $i$=$x$ or $i$=$z$ depending on the control laws in eqs. (12, 14). Inserting eqs. (10, 11, 12, 14) in eq. (8) for state vector $\underline{s}_2$ yields then the nonlinear set of equations

$$\ddot{\underline{s}}_2 + K_d \dot{\underline{s}}_2 + (K_p - N)\underline{s}_2 = K_p \underline{s}_{r2} \,, \tag{17}$$

where $N$ comprises the nonlinearity in the system, the components from $\underline{s}_{r2}$ are extracted from $\underline{s}_r$ and $K_p$=$diag\{k_{pi}, k_{py}\}$ and $K_d$=$diag\{k_{di}, k_{dy}\}$ denote the gain matrices.

Besides the Sun vector control, the rate around the sunline has to be controlled. This requires the knowledge of angular rates, and next, an estimation algorithm is outlined.

*Estimation of angular rates.* Rewriting the modified Euler equation (eqs. (5, 6)) yields

$$\underline{a} + \underline{b}\omega_l + \underline{c}\omega_l^{\,2} = \underline{0} \tag{18}$$

with

$$\underline{a} = -\ddot{\underline{s}} + \dot{\tilde{\underline{s}}}\tilde{\underline{s}}\underline{s} + \tilde{\underline{s}}\underline{\tau}_t \tag{19a}$$

$$\underline{b} = -\tilde{\underline{s}}(I^{-1}(\tilde{\underline{\omega}}_t I \underline{s} + \tilde{\underline{s}}(I\underline{\omega}_t + \underline{h})) + \dot{\underline{s}}) \tag{19b}$$

$$\underline{c} = -\tilde{\underline{s}} I^{-1} \tilde{\underline{s}} I \underline{s} \;. \tag{19c}$$

Eq. (18) can be interpreted as a vector equation with unknown scalar $\omega_l$. All known vectors $\underline{a}$, $\underline{b}$, $\underline{c}$ are in one plane, and it can be shown that they are always perpendicular towards Sun vector $\underline{s}$.

The question here is: Under which circumstances can eq. (18) uniquely be solved for $\omega_l$? The possible cases are discussed now in principle, neglecting the details of the actual implementation.

Case 1: The vectors are not colinear.
In this case, $\omega_l$ can uniquely be solved by multiplying eq. (18) from the left with the transposed of a vector standing perpendicular to $\underline{c}$ resulting in

$$\omega_l = -\frac{(\tilde{\underline{s}}\underline{c})^T \underline{a}}{(\tilde{\underline{s}}\underline{c})^T \underline{b}} \,. \tag{20}$$

As an alternative, vector $\underline{a}$ instead of vector $\underline{c}$ can be cancelled out. A unique solution can then still be found for $\omega_l$, when $\omega_l$ cannot be zero.

Case 2: The vectors are (almost) colinear.

Case 2.1: No vector vanishes.

Eq. (18) cannot uniquely be solved. Multiplying eq. (18) from the left with the transposed of a vector $\underline{l}$ which is optimal from a numerical point of view yields a quadratic equation and thus two possible solutions for $\omega_l$:

$$\omega_{l1,2} = -\frac{\underline{l}^T\underline{b}}{2\underline{l}^T\underline{c}} \pm \sqrt{\left(\frac{\underline{l}^T\underline{b}}{2\underline{l}^T\underline{c}}\right)^2 - \frac{\underline{l}^T\underline{a}}{\underline{l}^T\underline{c}}} \qquad (21)$$

Case 2.2: One vector vanishes.

This can happen in steady state, where non-spherical mass distribution is assumed:

a) Vector $\underline{c}$ vanishes when the Sun vector $\underline{s}$ coincides with one of the principal axes, and vector $\underline{b}$ does not vanish when $\underline{s}$ and $\underline{h}$ are not parallel. Then, the solution is obtained by multiplying eq. (18) from the left with a transposed suitable vector $\underline{l}$:

$$\omega_l = -\frac{\underline{l}^T\underline{a}}{\underline{l}^T\underline{b}}. \qquad (22)$$

b) Vector $\underline{b}$ vanishes when $\underline{s}$ and $\underline{h}$ are parallel, and vector $\underline{c}$ does not vanish when Sun vector $\underline{s}$ does not coincide with one of the principal axes. Then, $\omega_l$ can no longer uniquely be determined, and from eq. (18) two solutions are obtained:

$$\omega_{l1,2} = \pm\sqrt{\frac{\underline{l}^T\underline{a}}{\underline{l}^T\underline{c}}}. \qquad (23)$$

The sign of $\omega_l$ can be determined in the following way. In steady state, the Euler equation (1) expressed with the 'unknown' $\omega_l$ (eq. (4)) reduces to

$$I\underline{s}\dot{\omega}_l + \tilde{\underline{s}}I\underline{s}\omega_l^2 = \underline{\tau}_c, \qquad (24)$$

in which only the square of $\omega_l$ enters. Solving eq. (24) for $\dot{\omega}_l$ yields

$$\dot{\omega}_l = \frac{\underline{s}^T\underline{\tau}_c}{\underline{s}^T I\underline{s}}. \qquad (25)$$

Knowing the magnitude $|\omega_l|$ from eq. (23) and the derivative of $\omega_l$ from eq. (25), the sign of $\omega_l$ is determined uniquely, if $|\omega_l|$ is 'sufficiently' far from zero, as shown in table 1. But this is no restriction in practice, because noisy data prohibits a reliable computation in the zero-region of $|\omega_l|$ anyway, and with sufficient waiting time the zero-region is avoided.

| | $\dot{\omega}_l > 0$ | $\dot{\omega}_l < 0$ |
|---|---|---|
| $d\lvert\omega_l\rvert/dt > 0$ | + | - |
| $d\lvert\omega_l\rvert/dt < 0$ | - | + |

Table 1: Sign of $\omega_l$ depending on $\dot{\omega}_l$ and $d|\omega_l|/dt$.

Once $\omega_l$ is known in steady state at a certain time instant completely, it can continously be computed by integrating eq. (25). The advantage is, that less problems are expected in the zero-region due to the low pass filter effect of the integrator.

Case 2.3: All vectors vanish.

No solution can be obtained, for instance in steady state when $\underline{s}$ and $\underline{h}$ are parallel and $\underline{s}$ coincides with one of the principal axes.

*Sunline rate control.* In steady state condition, i.e. $\underline{\omega}_t = \underline{0}$, eq. (24) can be written using eqs. (7, 9) as

$$\underline{s}\dot{\omega}_l = \underline{T}_l. \qquad (26)$$

A simple proportional control law with positive gain $k_p$ and reference signal $\omega_{ref}$,

$$\underline{T}_l = -k_p(\omega_l - \omega_{ref})\underline{s}, \qquad (27)$$

gives (after inserting eq. (27) in eq. (26) and multiplying the result with $\underline{s}^T$) a stable, linear system:

$$\dot{\omega}_l + k_p(\omega_l - \omega_{ref}) = 0. \qquad (28)$$

As an example, figure 5 shows the result of a Sun vector control for a satellite with inertia matrix *I=diag{12269, 2077, 11788} kgm²* and negligible products of inertia. The solid line shows the components of the simulated Sun vector, where as the long dashed line shows the Sun reference vector.

Even though the Sun is out of the sensor's FOV at simulation start, the satellite is tilted and the Sun vector controller rotates the Sun vector to a principal (z-) axis. The Sun reference vector reveals from about t=1200s until t=3600s a bias from the principle axis in order to estimate the angular rates, see case 2.2, b).

Figure 6 shows the simulated angular rates (solid line) and the estimated angular rates (long dashed). The little discrepancy comes from the fact, that onboard the inertia matrix has 20% greater moments of inertia than in the simulation.

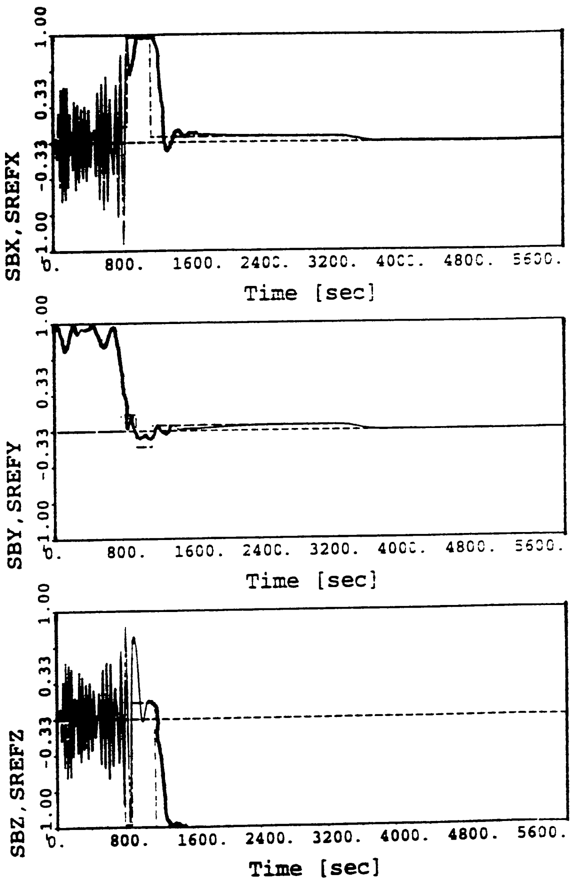


Figure 5: Typical Sun vector control plot.

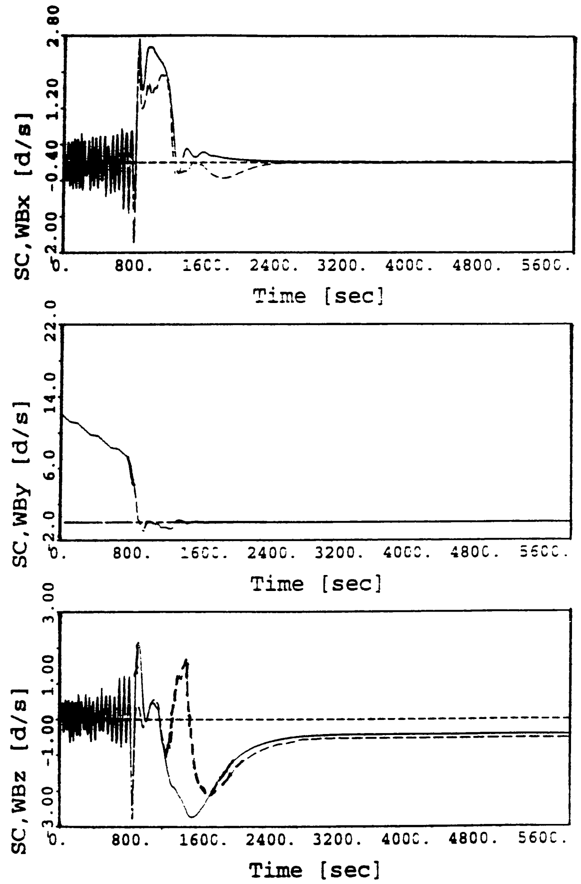


Figure 6: Typical sunline rate control plot.

*4.2 Earth Acquisition Mode*

The same concept as for the SAM, only a time variant Sun reference vector derived from orbit propagation is used. The satellite rotates then about the sunline on an onboard computed conus, on which Earth presence is guaranteed to be found. Then, the attitude is completely determined and a 3-axis-stabilized control system is activated.

*4.3 Apogee Boost Mode*

During the apogee boost mode, the satellite has to be 3-axis stabilized. Because of the location of the apogee boost motor (-z-side), the Earth sensor (aligned along the +z-axis) cannot be used for attitude measurement purposes, see figure 4, and therefore the only direct attitude information is delivered from the 2-axis Sun sensor. Generally, there are two possibilities to obtain 3-axis attitude information during this operational phase:

1. Implementation of an additional low-cost, single-axis Earth sensor along the satellite x-axis. The boost maneuver will then be performed in an Earth-oriented attitude.

2. Use of gyro(s). At least one single-axis gyro in addition to the Sun sensor is necessary, in order to obtain 3-axis attitude information. The boost maneuver can then be performed with respect to an inertially fixed reference attitude.

In the former case, provisions have to be made that Sun and Earth sensor measurements are not colinear. In the latter case, i.e. when gyros are used, the 3-axis attitude is derived by a strap-down algorithm, which is outlined subsequently for the case of one single-axis gyro.

Step 1: Compute a small rotation vector $\underline{\varphi}$ during the instantaneous sample time interval in the way described below. Let $\underline{s}(k)$, $\underline{s}(k-1)$ denote the Sun vector at time $k$ and $k-1$, $\underline{g}$ the gyro (unit-)input axis, and $\delta$ the measured gyro rate around the axis $\underline{g}$ integrated over one sample interval (figure 7):

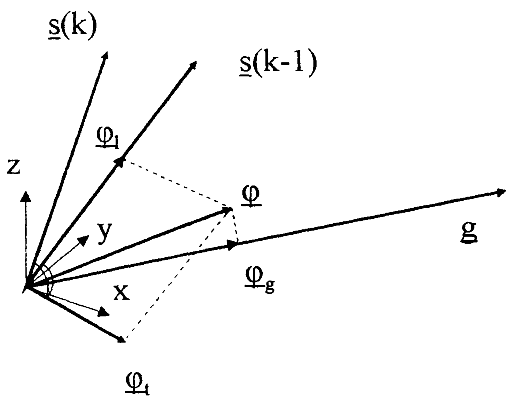


Figure 7: Decomposition of Sun vector $\underline{\varphi}$ .

During a sample interval, the satellite's behaviour can be considered as a rotation $|\underline{\varphi}|$ about a time invariant rotation axis $\underline{\varphi}$. Here, the rotation is very small and linear. Then, the rotation vector $\underline{\varphi}$ can be decomposed into

$$\underline{\varphi} = \underline{\varphi}_l + \underline{\varphi}_t \, , \qquad (29)$$

see figure 7, where

$$\underline{\varphi}_t = \underline{\tilde{s}}(k-1)\underline{s}(k) \qquad (30)$$

is a transversal component with respect to the measured Sun vectors $\underline{s}(k)$, and $\underline{s}(k-1)$ and

$$\underline{\varphi}_l = \underline{s}(k-1)x \qquad (31)$$

an unknown component along $\underline{s}(k-1)$ of length $x$. Component $\underline{\varphi}_l$ can be computed via the rate integrating gyro, which measures $\delta(k)$, the component of $\underline{\varphi}$ along the axis $\underline{g}$,

$$\delta(k) = \underline{g}^T \underline{\varphi} \, , \qquad (32)$$

by substituting eqs. (29-31) in eq. (32), to yield

$$\underline{\varphi} = \underline{\tilde{s}}(k)\underline{s}(k-1) + \underline{s}(k-1)\frac{\delta(k) - \underline{g}^T \underline{\tilde{s}}(k)\underline{s}(k-1)}{\underline{g}^T \underline{s}(k-1)} \, . \qquad (33)$$

Step 2: Compute from $\underline{\varphi}$ the corresponding small quaternion $\Delta q$, and then, by quaternion multiplication, the actual (large angle) quaternion $q(k)$ with respect to the inertial reference attitude:

$$q(k) = q(k-1) o \Delta q \qquad (34)$$

Step 3: Apply a correction on the result $q(k)$, corresponding to the attitude information, that can be measured directly by the Sun sensor.

From eq. (33) it is obvious, that $\underline{g}^T \underline{s}$ must be nonzero during the whole maneuver. In the case of several gyros, this is always fullfilled. However, in the 'minimal' configuration, when only one gyro is used, this condition must be considered for the gyro orientation and/or the launch window. For midnight-launches, the gyro will be oriented along the satellite x-axis.

## 5. CONCLUSIONS

An attitude control concept was proposed which requires no gyro during acquisition modes and a single gyro only during the apogee boost mode. This means, that once a satellite is in geosynchronous orbit, it is completely indpendent from gyro measurements, because the normal mode and the station keeping mode are performed without gyros anyway. If an additional Earth sensor is implemented, the whole mission from launch to deorbiting can be performed without gyros.

## 6. REFERENCES

[1] 'AOCS 3000 for the New Generation of 3-Axis Stabilized Communication Satellites'
M. Surauer, R. Hartmann, A. Brauch, K. Miltenberger, H. Schmid
IFAC Aerospace Symposium,
Palo Alto, California, 1994

[2] 'Advanced Attitude and Orbit Control Concepts for 3-Axis Stabilized Communication and Application Satellites'
M. Surauer, H. Bittner, W. Fichter, H. D. Fischer
12th IFAC Symposium on Automatic Control in Space,
Ottobrunn, Germany, 1992.